J. Phys. Chem. 1994, 98, 11181−11192

Liquid−Vapor Equilibria of Polar Fluids from a van der Waals-like Theory

Carlos Vega,* Santiago Lago, and Benito Garzón

Departamento de Química-Física, Facultad de Ciencias Químicas, Universidad Complutense, 28040 Madrid, Spain

Received: March 29, 1994; In Final Form: July 14, 1994[⊗]

A van der Waals-like theory of quadrupolar and dipolar linear fluids is presented. The reference system consists of a hard polar fluid, and attractive forces are considered through the mean field approximation. The effect of polar forces on liquid−vapor equilibria and on critical properties is analyzed for a number of molecular elongations. Trends as predicted by the theory are compared with computer simulations of linear polar fluids, and good agreement is found. Polar forces increase the critical temperature and acentric factor of a fluid. Quadrupole moment increases the critical density of a fluid. However, high dipole moments decrease critical densities. Deviations from the principle of corresponding states are analyzed. Polar forces and molecular elongation provoke a broadening of the coexistence curve and an increase of the slope of the vapor pressure curve when reduced by their critical magnitudes. The presented treatment, being quite simple, describes most of the main features of vapor−liquid equilibria of linear polar fluids.

I. Introduction

It is a century now since van der Waals proposed his equation of state.[1] A consequence of this equation is that all fluids follow the same equation of state when reduced by their critical magnitudes. That constitutes the principle of corresponding states which was later formulated on a molecular basis.[2] Although this principle holds quite well for spherical and almost spherical molecules, important deviations were found for molecules having a nonspherical shape or presenting a multipole (dipole or quadrupole) moment. Early attempts to account for these deviations from statistical mechanics grounds were formulated.[3,4] They were especially successful in the description of the effect of polar forces on spherical-shaped models.[5] The past two decades were quite active in developing an understanding of the role of molecular shape on phase equilibria. van der Waals-like theories,[6] perturbation theories,[7−10] or even computer simulation[11] have provided a clear understanding of the role of molecular shape on phase equilibria. The situation is less satisfactory for nonspherical polar fluids although some recent progress should be mentioned.

Integral equations are now being solved for a number of linear polar models,[12] and progress in the field through this line may be anticipated. Perturbation theories have recently been developed for linear polar fluids, and the consequences have not completely been explored yet.[13−17] Simultaneously, a number of simulation studies concerning dipolar and quadrupolar linear fluids have been performed.[18,19] Quite recently, it has become possible to easily obtain liquid−vapor equilibria by computer simulation through the so-called Gibbs ensemble methodology.[20] This new route is just being explored. In fact, Dubey et al.[21] have presented simulation results for linear dipolar fluids, and we have recently performed a very comprehensive simulation study of quadrupolar linear Kihara fluids.[22] A similar study for a quadrupolar two-center Lennard-Jones model has recently been performed by using the NPT+ test particle method.[23] These studies can be considered as examples of what may be learned in the near future on vapor−liquid equilibria of linear polar fluids.

Our approach in this work is however slightly different. Our aim is to show the simplest theory that can account for the effect of both shape and polarity on phase equilibria. Rigby[6] proposed a van der Waals-like treatment of linear nonpolar fluids. The idea is to take a hard convex body as reference system and to include the effect of dispersion forces through a mean field term. Here we shall follow this idea. We shall take a hard polar system as reference state, and we shall include dispersion forces through a mean field term. For describing the reference hard polar fluid we shall use a simple perturbation theory which has provided satisfactory agreement with computer simulation for these systems.[14−17] This theory is a compromise between accuracy and simplicity, which becomes an important factor in phase equilibria studies. The purpose of this paper is to provide a general view of the role played by shape and polarity on phase equilibria by using a very simple treatment. In particular, the effect of the quadrupole or dipole moment on critical properties of a linear fluid is analyzed. Deviations from the principle of corresponding states due to both shape and polarity and the coupling between these two factors will also be considered. We pay some attention to the study of the effect provoked by a given quadrupole or dipole on molecules with different elongations. Although dipole and quadrupole moments provoke the same effect on some critical properties, an analysis of some differences is also performed. A clear understanding of the role of polarity and shape on phase equilibria is important since most of more common fluids have both nonspherical shape and polar forces.

The scheme of the paper is as follows. In section II a perturbation theory for hard polar fluids is presented. Section III describes the van der Waals-like treatment that will be used in this work. In section IV results of liquid−vapor equilibria for linear nonpolar fluids, linear quadrupolar fluids, and linear dipolar fluids are presented. In section V we present a simplified theoretical treatment that provides analytical formulas for the effect of polar forces on critical properties. Finally, section VI summarizes the main conclusions of this work.

II. Hard Polar Fluids

In this section we shall study a linear hard spherocylinder (HSP) with an embedded point dipole or quadrupole. The shape

---

* Author for correspondence.

[⊗] Abstract published in *Advance ACS Abstracts*, October 1, 1994.

0022-3654/94/2098-11181$04.50/0

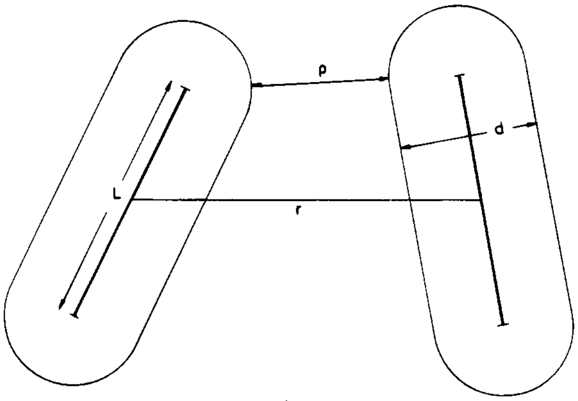

Figure 1. Geometry of a hard spherocylinder. The meaning of L, d, and ϱ is illustrated.

of the HSP is defined by $L^* = L/d$, which is the ratio of the bond length L to the molecular diameter d as illustrated in Figure 1. The dipole–dipole u^{DD} or quadrupole–quadrupole u^{QQ} potentials are given by

$$u^{\mathrm{DD}} = (\mu^2/r^3)(s_1s_2c - 2c_1c_2) \tag{1}$$

$$u^{\mathrm{QQ}} = (3Q^2/4r^5)[1 - 5(c_1{}^2 + c_2{}^2) - 15c_1{}^2c_2{}^2 + 2(s_1s_2c - 4c_1c_2)^2] \tag{2}$$

where μ and Q stand for the dipole and quadrupole moment, $c_i = \cos\theta_i$, $s_i = \sin\theta_i$ and $c = \cos(\phi_1 - \phi_2)$. In eqs 1 and 2 the polar axis is the one connecting the center of mass of both molecules. We shall use reduced multipole moments defined as

$$Q^{*2} = Q^2/(\epsilon d^5) \tag{3}$$

$$\mu^{*2} = \mu^2/(\epsilon d^3) \tag{4}$$

where ϵ is an arbitrary unit of energy and d is the diameter of the hard spherocylinder (see Figure 1). Therefore, the total pair potential is given for a quadrupolar hard spherocylinder (HSPQ) by

$$u^{\mathrm{HSPQ}} = u^{\mathrm{HSP}} + u^{\mathrm{QQ}} \tag{5}$$

and for a dipolar hard spherocylinder (HSPD) by

$$u^{\mathrm{HSPD}} = u^{\mathrm{HSP}} + u^{\mathrm{DD}} \tag{6}$$

The ideal dipole or quadrupole aligned with the molecular axis is situated on the center of mass of the molecule. All our discussions and conclusions refer to that case.

Boublik has recently developed a perturbation theory for hard ellipsoids with a quadrupole[14,15] (HEQ) or dipole[16] (HED). This perturbation theory has been extended to HSPQ fluids with good results.[17] We briefly summarize the theory and refer the reader to the original papers for details.[14–17] In this perturbation theory the HSP is taken as the reference system, and the perturbation terms up to third order are evaluated. To accelerate the convergence of perturbation series, a Padé approximant is used.[24] Structure of the hard reference fluid is needed to evaluate the perturbation terms. This is, in general, unknown or difficult to obtain so that the Parsons[25] approximation is used. That means that the pair correlation function $g(r,\omega_1,\omega_2,y)$ is approximated by $g_{\mathrm{HS}}(r/D(\omega_1,\omega_2),y)$ where g_{HS} is the radial distribution function of hard spheres and $D(\omega_1,\omega_2)$ in the distance between the centers of mass when the two molecules are at contact for the relative orientation ω_1,ω_2. The packing fraction y is defined by

$$y = nV_{\mathrm{m}} \tag{7}$$

$$V_{\mathrm{m}} = \frac{\pi}{6}d^3\left(1 + \frac{3}{2}L^*\right) \tag{8}$$

where n is the number density of the fluid and V_{m} is the molecular volume of the HSP. Parsons's approximation uncouples orientational and radial coordinates, and each perturbation term reduces to an orientational average of a certain function of the angular part of the polar potential and a radial[14–17] integration of a certain function of g_{HS}. The free energy for HSPQ is given by[17]

$$A^{\mathrm{HSPQ}} = A^{\mathrm{HSP}} + A^{\mathrm{Q}} \tag{9}$$

$$A^{\mathrm{Q}} = A^{\mathrm{Q}}_{1\mathrm{A}} + A^{\mathrm{Q}}_{2\mathrm{A}}(1 - (A^{\mathrm{Q}}_{3\mathrm{A}} + A^{\mathrm{Q}}_{3\mathrm{B}})/A^{\mathrm{Q}}_{2\mathrm{A}})^{-1} \tag{10}$$

where A^{HSPQ} is the free energy of the quadrupolar model, A^{HSP} is the free energy of the hard spherocylinder, and A^{Q} is the quadrupolar contribution to the free energy. Defining $n^* = nd^3$, then $A^{\mathrm{Q}}_{1\mathrm{A}}$, $A^{\mathrm{Q}}_{2\mathrm{A}}$, $A^{\mathrm{Q}}_{3\mathrm{A}}$, and $A^{\mathrm{Q}}_{3\mathrm{B}}$ are given by

$$A^{\mathrm{Q}}_{1\mathrm{A}}/NkT = (3/2)\pi n^*(Q^{*2}/T^*)I_{\mathrm{Q}}(L^*)\, a_{\mathrm{Q}}(y) \tag{11}$$

$$A^{\mathrm{Q}}_{2\mathrm{A}}/NkT = -\pi n^*(9/16)(Q^{*4}/T^{*2})J_{\mathrm{Q}}(L^*)\, b_{\mathrm{Q}}(y) \tag{12}$$

$$A^{\mathrm{Q}}_{3\mathrm{A}}/NkT = \frac{9\pi n^*}{64}(Q^{*6}/T^{*3})K_{\mathrm{Q}}(L^*)\, c_{\mathrm{Q}}(y) \tag{13}$$

$$A^{\mathrm{Q}}_{3\mathrm{B}}/NkT = \frac{9}{16}\pi^2 n^{*2}(Q^{*6}/T^{*3})\frac{1}{[(V_{\mathrm{m}}/d^3)/(\pi/6)]^5}z_{\mathrm{Q}}(y) \tag{14}$$

where I_{Q}, J_{Q}, and K_{Q} are geometrical quantities obtained by integration and depending on the particular shape of the considered model.[17,26] The reduced temperature is defined as $T^* = T/(\epsilon/k)$ where ϵ is some arbitrary unit of energy. Expressions for $a_{\mathrm{Q}}(y)$, $b_{\mathrm{Q}}(y)$, $c_{\mathrm{Q}}(y)$, and $z_{\mathrm{Q}}(y)$ are given in eqs 32–34 of ref 17. These functions can be obtained by numerical integration of radial distribution function of hard spheres divided by the appropriate power of the distance between the centers of mass. Values of I_{Q}, J_{Q}, and K_{Q} for HSP have been previously reported in refs 17 and 26. The theory may be extended to HSPD fluids.[26] Now I_{D} and K_{D} are zero so that $A_{1\mathrm{A}}$ and $A_{3\mathrm{A}}$ vanish. A^{HSPD} is given by

$$A^{\mathrm{HSPD}} = A^{\mathrm{HSP}} + A^{\mathrm{D}} \tag{15}$$

$$A^{\mathrm{D}} = A^{\mathrm{D}}_{2\mathrm{A}}(1 - A^{\mathrm{D}}_{3\mathrm{B}}/A^{\mathrm{D}}_{2\mathrm{A}})^{-1} \tag{16}$$

The $A_{2\mathrm{A}}$ term is given by

$$A^{\mathrm{D}}_{2\mathrm{A}}/NkT = -\pi\, n^*(\mu^{*4}/T^{*2})J_{\mathrm{D}}(L^*)\, b_{\mathrm{D}}(y) \tag{17}$$

The determination of $A^{\mathrm{D}}_{3\mathrm{B}}$ requires three-body distribution functions. Boublik[27] has evaluated this term for dipolar ellipsoids by using the superposition approximation. In this work $A^{\mathrm{D}}_{3\mathrm{B}}$ of the HSPD model is taken from the corresponding dipolar hard ellipsoid model of the same length to breadth ratio. With this approximation $A^{\mathrm{D}}_{3\mathrm{B}}$ is given by[27]

$$A^{\mathrm{D}}_{3\mathrm{B}}/NkT = \frac{4}{3}\pi^2 n^{*2}(\mu^{*6}/T^{*3})(0.0236)\frac{(1 + 2y + 2y^2)}{(L^* + 1)^{1.063}} \tag{18}$$

Values of J_{D} for $L^* < 1$ were determined numerically by using

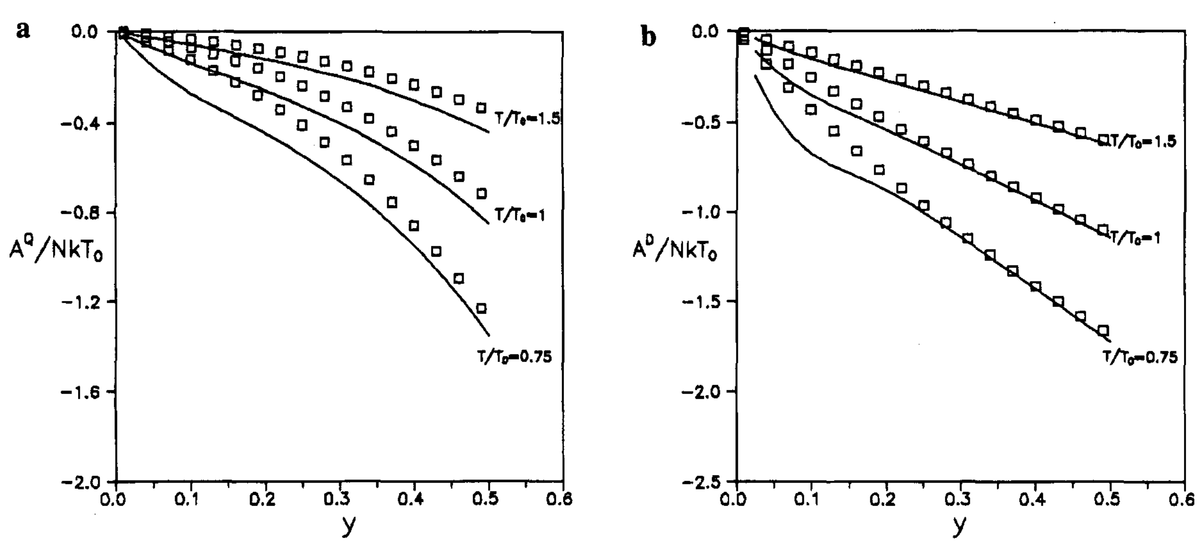

Figure 2. Polar contribution to the free energy of a linear model with $L^* = 0.505$ as obtained from the theory of this work (symbols) and from simulation results of a two-center Lennard-Jones model[19,30] (lines). Free energy is plotted versus the packing fraction y (eq 7). The critical temperature of the nonpolar model of the same elongation is denoted as T_0. Values of T_0 are given in Tables 1 and 2. For the two-center Lennard-Jones model T_0 was taken from ref 30. (a) Quadrupolar free energy A^Q for a model with $Q^{*}_{eq}{}^2$ 1.588 (see eq 34 for $Q^{*}_{eq}{}^2$). (b) Dipolar free energy A^D for $\mu^{*}_{eq}{}^2 = 2.932$ (see eq 35 for $\mu^{*}_{eq}{}^2$).

the Conroy[28] integration method. The obtained values of J_D were fitted to a empirical polynomial which is given for $L^* < 1$ by

$$J_D = 0.6666 - 1.2377L^* + 1.7814L^{*2} - 1.8447L^{*3} + 1.1584L^{*4} - 0.3158L^{*5} \quad (19)$$

Definition of the function $b_D(y)$ and empirical fits to their computed values were reported in ref 26.

The residual free energy of the hard spherocylinder system A^{HSP} is obtained from integration of the EOS of hard convex bodies proposed by Nezbeda.[29] To obtain the total part, an ideal gas term must be added. The final expression is

$$A^{HSP} = [\ln(y) - 1] + \frac{y(5\alpha^2 - \alpha - y(7\alpha^2 - 5\alpha + 1))}{(1 - y)^2} + (5\alpha^2 - 4\alpha - 1)\ln(1 - y) \quad (20)$$

$$\alpha = \frac{(L^* + 2)(L^* + 1)}{(3L^* + 2)} \quad (21)$$

where α is the nonsphericity parameter of the HSP model. Let us mention that Parsons[25] has proposed another expression for A^{HSP} which is especially accurate for very elongated molecules. For the elongations considered in this work eq 20 yields better results.

Equations 9–21 consistute the route to obtain $A_{HSPQ,HSPD}$. These equations have been tested by comparing their predictions with Monte Carlo results, and the agreement was found to be satisfactory.[17] As a further check, the polar contribution to the Helmholtz free energy (A^Q or A^D) determined from the theory of this work for a model with $L^* = 0.505$ is compared to that obtained from simulation for a two-center Lennard-Jones model with the same elongation. Saager and Fischer[30,31] have performed a comprehensive study of two-center Lennard-Jones polar models with $L^* = 0.505$ so that the polar contribution to the free energy is now well-known for this model. The comparison is shown in Figure 2. The theory accounts for the main features of the contribution of polar forces to the free energy. A drawback of our working expressions for $A_{HSPQ,HSPD}$ is that they predict liquid–vapor equilibria even in the absence of dispersion forces. For dipolar hard spheres ($L^* = 0$) such liquid–vapor transition has not been found in computer simulations.[32]

The main advantage of the theory is to provide a reasonable description of the behavior of hard linear polar fluids while keeping a simple form. This is especially useful in the context of phase equilibria where a fast determination of thermodynamic properties at any thermodynamic state is required. Certainly, one could use more sophisticated theories to describe hard polar fluids, as for instance integral equation theory.[33] However, if the interest is focused on the effect of the dipole or quadrupole moment on phase equilibria, the proposed treatment may be enough for a qualitative description of the trends. In fact, this treatment has recently been applied to analyze the effect of a quadrupole moment on liquid–solid equilibria, and an explanation of the high triple point of carbon dioxide was obtained.[34] We have also shown the effect of a dipole or quadrupole moment on the isotropic–nematic equilibria of long linear models.[26] In this work we study the effect of the dipole or quadrupole moment on the liquid–vapor equilibria of a linear fluid.

III. van der Waals Model of Polar Fluids

A hard polar model is not certainly a complete model of a liquid. Although short-range forces accounting for the molecular shape are included and long-range attractive forces arising from multipolar moments are considered, an inclusion of attractive dispersion forces is still needed. A simple way to do it is to use the van der Waals treatment so that each molecule feels a uniform background due to the presence of attractive dispersion forces. That is equivalent to incorporate a term in the free energy which is linear in density. Whereas this is not exact, it constitutes a simple way of incorporating attractive forces and it will be adopted in this work. The free energy of a molecule according to all this approximations is given by

$$A/N = A^{HSPQ,HSPD}/N - an \quad (22)$$

The equation of state following from eq 22 is

$$p = p^{HSPQ,HSPD} - an^2 \quad (23)$$

Equations 22 and 23 are the basic equations of this work. The original van der Waals (VDW) EOS was quite useful for describing real fluids. However, for some time it was not easy to establish a link between a statistical thermodynamic theory and the VDW EOS. The development of perturbation theories allowed this link. At present, it is possible to derive the van der Waals EOS starting from first principles and by doing some well-defined approximations.[35] It would be useful to have such a derivation for our extension of the VDW EOS to polar fluids. This derivation may be done in the following way. Let us assume that the pair potential between two linear molecules is given by the Kihara potential[36] plus a multipolar term (dipolar or quadrupolar):

$$u(\varrho) = 4\epsilon[(\sigma/\varrho)^{12} - (\sigma/\varrho)^{6}] + u^{\mathrm{QQ,DD}} \qquad (24)$$

In eq 24 ϱ is the shortest distance between the molecular cores. For our linear model the molecular core will be taken as a linear rod of length L, or if σ is used as unit of length $L^* = L/\sigma$. Let us divide the full pair potential into a reference u_0 and a perturbation part u_1:

$$u = u_0 + u_1 \qquad (25)$$

We shall take for the reference system u_0:

$$u_0(\varrho) = 4\epsilon[(\sigma/\varrho)^{12} - (\sigma/\varrho)^{6}] + u^{\mathrm{QQ,DD}} \qquad \varrho < \sigma \qquad (26)$$

$$u_0(\varrho) = u^{\mathrm{QQ,DD}} \qquad \varrho > \sigma \qquad (27)$$

The perturbation term can be easily obtained from eqs 25–27. The free energy of the full potential is given up to first order in the perturbation by

$$A/N = A_0/N + A_1/N \qquad (28)$$

$$A_1/N = n/2\int_{\sigma}^{\infty} 4\epsilon[(\sigma/\varrho)^{12} - (\sigma/\varrho)^{6}]g_0(\varrho)\, S_{c+\varrho+c}(\varrho)\, \mathrm{d}\varrho \qquad (29)$$

where $g_0(\varrho)$ is the surface to surface average correlation function of the reference system given by eqs 26 and 27 and $S_{c+\varrho+c}(\varrho)$ is the surface averaged over all the relative orientations of the body generated by the center of mass of molecule two when moving around molecule one at constant ϱ. Convex body geometry[37] was used in deriving eq 29. Now we shall relate the properties of the reference system to those of a hard polar system with a hard diameter $d = \sigma$. We shall also neglect correlations as usual in mean field treatments. These two approximation may be written as

$$A_0 = A^{\mathrm{HSPQ,HSPD}}(d{=}\sigma) \qquad (30)$$

$$g_0(\varrho) = 1 \qquad (31)$$

According to the approximation of eq 31 and using convex body geometry, A_1 may be written as

$$a = \pi\epsilon\sigma^3[(6/55)L^{*2} + (6/5)L^* + (16/9)] \qquad (32)$$

$$A_1/N = -an \qquad (33)$$

By adding together eq 30 and eq 33, we recover our previous eq 22. Throughout this work the van der Waals constant a will be given by eq 32. The approximations contained in eq 22 are now clear. The first approximation is the truncation of the perturbation expansion at first order. The other two approximations are given by eqs 30 and 31. It is clear that this simplified theory can only account for qualitative trends of the model given by eq 24 and that no quantitative agreement may be expected. Since our intention here is to explore trends in phase equilibria of linear polar molecules, some of the main features can probably be illustrated from this van der Waals-like treatment. Eventually, a more sophisticated treatment of dispersion forces as for instance that proposed by Saager et al. may be incorporated in the theory.[38] It is interesting to stress here that our van der Waals-like equation of state has four independent variables, namely, ϵ, σ, L^*, and Q^* (or μ^*).

Taking σ and ϵ from eq 24 as unit of length and energy, respectively, then the independent variables are L^* and Q^* (or μ^*). If L^* is fixed, it is possible to analyze the effect of Q^* on phase equilibria. In this way we learn about the effect of quadrupole on phase equilibria of a given model. Another possibility is to fix Q^* and to see the effect at different equations. Although we have used eq 3 to define Q^* (with $d = \sigma$), it should be recognized that the way of reducing a quadrupole moment is not unique. A general problem when comparing two polar models with different elongations is how to define the reduced quadrupole (dipole). One would like to have an "equivalent" quadrupole (dipole) for both elongations so that one could evaluate the effect of the same "equivalent" quadrupole at two different elongations. The problem arises from the fact that the concept of "equivalent" quadrupole is ill-defined. Even admitting the arbitrary character of the concept "equivalent" quadrupole, we found Q^* as defined by eq 3 not particularly useful. We propose now a new way of reducing the quadrupole or dipole moment which will be denoted as Q^*_{eq} and μ^*_{eq}, respectively. They are defined by the expressions

$$Q^*_{\mathrm{eq}}{}^2 = Q^2/kT_0(V_{\mathrm{m}})^{5/3} \qquad (34)$$

$$\mu^*_{\mathrm{eq}}{}^2 = \mu^2/kT_0(V_{\mathrm{m}})^{3/3} \qquad (35)$$

where T_0 is the critical temperature of a model with the same elongation as the one under consideration but with no multipole moment. Note that for spheres the definition of eqs 34 and 35 is equivalent (except for a constant) to that of eqs 3 and 4. This way of reducing a dipole or quadrupole moment is similar (the difference being the presence of the factor kT_0 instead of ϵ in the denominator of eqs 34 and 35) to another recently proposed[22] which was found to be very useful in analyzing Gibbs ensemble data of molecules with different elongations. It is also similar to that proposed in refs 18 and 31, the difference being the use of the molecular volume instead of the inverse of the critical density of the nonpolar model in eqs 34 and 35.

In Figure 3 we present the polar contribution to the free energy along the critical isotherm of the nonpolar model for several elongations when $Q^*_{\mathrm{eq}}{}^2 = 3$ (Figure 3a) and when $\mu^*_{\mathrm{eq}}{}^2 = 3$ (Figure 3b). The surprising result is that A^{Q} does not depend significantly on L^* when the definition of eq 34 is used. However, A^{D} depends on the molecular elongation, and the effect of the dipole seems to be larger for a spherical molecule than for an elongated model. These two facts will have consequences in the way quadrupole or dipole moment affect critical properties at different elongations. We shall return to this point later. Before leaving this section, it should be mentioned that the L^* dependence of A^{D} for fixed $\mu^*_{\mathrm{eq}}{}^2$ and packing illustrated in Figure 3b of this work is in agreement with that of ref 31. However, the L^* dependence of A^{Q} for a given $Q^*_{\mathrm{eq}}{}^2$ and y shown in Figure 3a is different from that found by Bohn et al.[18] (see Figure 7 of ref 18). The origin of this difference is unknown.

IV. Results

We shall present now the results obtained from eqs 22 and 23 for different models and elongations. We shall present first results for nonpolar models and then for quadrupolar and dipolar models. We shall finish with a comparison between the effect of a dipole and a quadrupole.

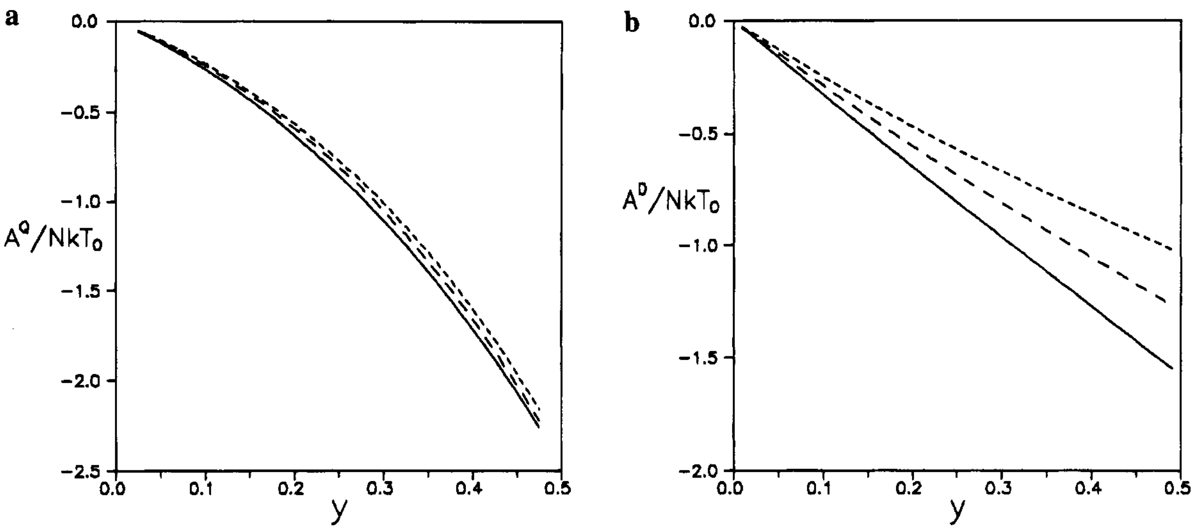

Figure 3. Polar contribution to the free energy obtained from the theory of this work versus packing fraction along the critical isotherm of a nonpolar model ($T = T_0$) with the same elongation. Solid line stands for $L^* = 0$, dashed line for $L^* = 0.3$, and short dashed line for $L^* = 0.8$. (a) Quadrupolar free energy A^Q for models with $Q^*_{\mathrm{eq}}{}^2 = 3$. (b) Dipolar free energy A^D for models with $\mu^*_{\mathrm{eq}}{}^2 = 3$.

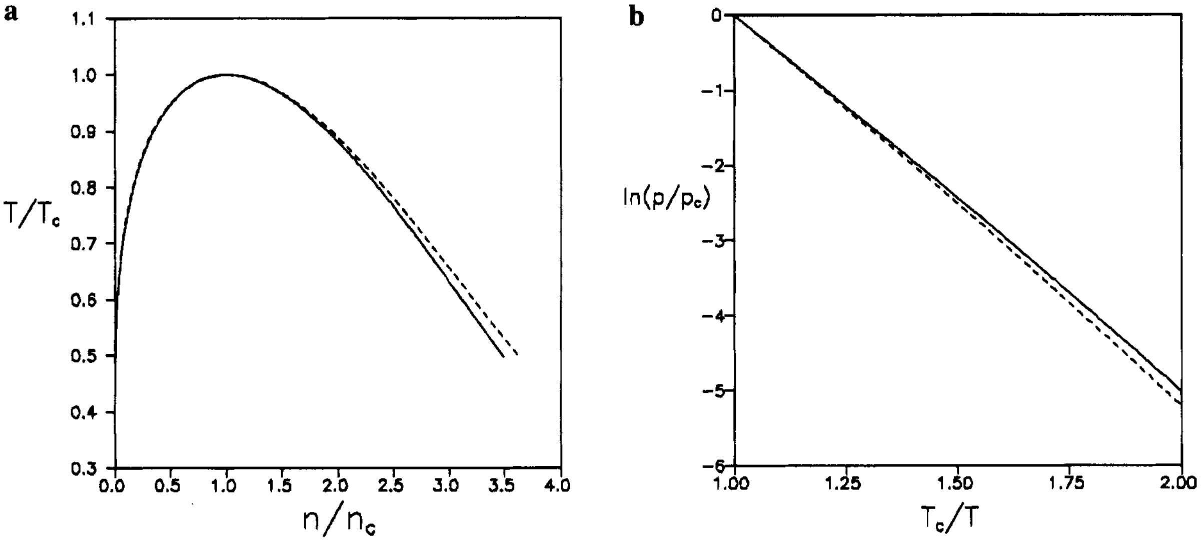

Figure 4. Corresponding states plot for linear nonpolar molecules obtained from the mean field treatment of this work: solid line, results for $L^* = 0$ (spherical model); dashed line, results for $L^* = 0.8$. (a) Coexistence densities of the liquid−vapor equilibria. (b) Vapor pressure.

(A) Nonpolar Models. For nonpolar models our treatment reduces to that previously proposed by Rigby[6] (except that a different EOS of hard convex bodies is used). In Figure 4 we present the vapor−liquid equilibria and vapor pressure curve in critical units for different elongations. Molecular anisotropy provokes a broadening of coexistence densities and increases the slope (in absolute value) of the vapor pressure curve. That was first described by Rigby. Deviations of corresponding states principle for the Kihara model predicted by the theory are smaller than the ones obtained from computer simulation in the Gibbs ensemble.[11] This is probably a consequence of the mean field approximation.

(B) Quadrupolar Models. We shall present now results for linear quadrupolar moments. In Figure 5a we show results for $L^* = 0.3$ and $Q^{*2} = 0$, 0.75, and 1.5 as obtained from the theory of this work. Recently, a very extensive study of liquid−vapor equilibria of quadrupolar Kihara fluids through Gibbs ensemble simulation[22] has been performed. In Figure 5 the theoretical predictions are shown along with the simulation results.[22] The theory does not correctly predict the critical temperature as expected, and this is again a consequence on the mean field treatment. The mean field approximation also causes differences of shape in the coexistence curve. However, the theory predicts an increase of the critical temperature, pressure, and density with the quadrupole, and this is in agreement with simulation. This is further illustrated in Table 1. Similar conclusions are obtained for other elongations. In Figure 6 we present results of the vapor pressure for the same models. Quadrupole decreases the vapor pressure curve at a given temperature. The slope at low temperatures of the vapor pressure curve is related to the enthalpy of vaporization through the Clausius−Clapeyron equation. Therefore, the theory predicts an increase of the enthalpy of vaporization due to the quadrupole.

In Figure 7a we present a corresponding states plot for the coexistence densities and in Figure 7b for vapor pressure. Results correspond to $L^* = 0.8$ and $Q^{*2} = 0$, 1.49, and 2.98, and for comparison results for $L^* = 0$ and $Q^{*2} = 0$ are also presented. We see how both molecular elongation and quadrupole moment provoke a broadening of the coexistence curve. Similarly, molecular elongation and quadrupole moment increase the slope (in absolute value) of the vapor pressure curve.

The acentric factor ω is defined through[39]

$$\omega = -\log[(p/p_c)_{T/T_c=0.7}] - 1 \qquad (36)$$

and can be easily evaluated from plots as the one shown in

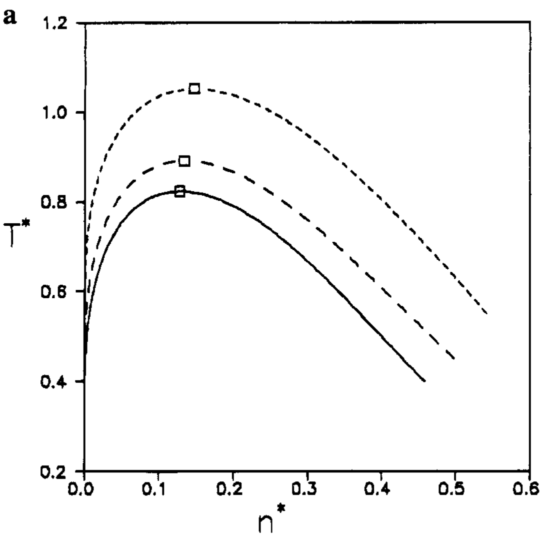

Figure 5. Coexistence densities of the liquid–vapor equilibria of linear quadrupolar models with $L^* = 0.3$. Solid line stands for $Q^{*2} = 0$, dashed line for $Q^{*2} = 0.75$, and short dashed line for $Q^{*2} = 1.5$. Open squares represent the critical point. (a) Results from the theory of this work. (b) Fit to the Gibbs ensemble simulation results of ref 22 and of ref 11 for a quadrupolar Kihara model.

TABLE 1: Critical Temperature T_c, Pressure p_c, and Density y_c of Linear Quadrupolar Models Obtained from the Mean Field Theory of This Work[a]

L^*	Q^{*2}	$Q^{*}_{eq}{}^{2}$	T_c	y_c	p_c	ω	$(A/NkT)_c$
0	0	0	1.006	0.130	0.090	−0.096	−3.15
0	0.558	1.632	1.123	0.139	0.108	0.047	
0	1.117	3.264	1.374	0.153	0.150	0.250	
0.3	0	0	0.823	0.129	0.050	−0.090	−3.16
0.3	0.75	1.442	0.891	0.135	0.057	0.026	
0.3	0.864	1.661	0.911	0.137	0.060	0.058	
0.3	1.5	2.883	1.052	0.148	0.076	0.254	
0.3	1.729	3.323	1.111	0.152	0.083	0.320	
0.6	0	0	0.716	0.125	0.032	−0.078	−3.19
0.6	1.222	1.721	0.795	0.133	0.039	0.071	
0.6	2.445	3.444	0.966	0.149	0.054	0.338	
0.8	0	0	0.666	0.123	0.025	−0.068	−3.21
0.8	1.492	1.770	0.742	0.131	0.031	0.079	
0.8	2.984	3.538	0.899	0.146	0.042	0.327	

[a] Critical density is defined in terms of the packing fraction defined as $y = nV_m$. $Q^{*}_{eq}{}^{2}$ is defined as $Q^2/(kT_0V_m{}^{5/3})$ where T_0 is the critical temperature of a nonpolar model with the same elongation. The critical pressure is given in $p/(\epsilon/\sigma^3)$ units. The acentric factor ω is also shown. Free energies at the critical point $(A/NkT)_c$ for nonpolar models are shown in the last column.

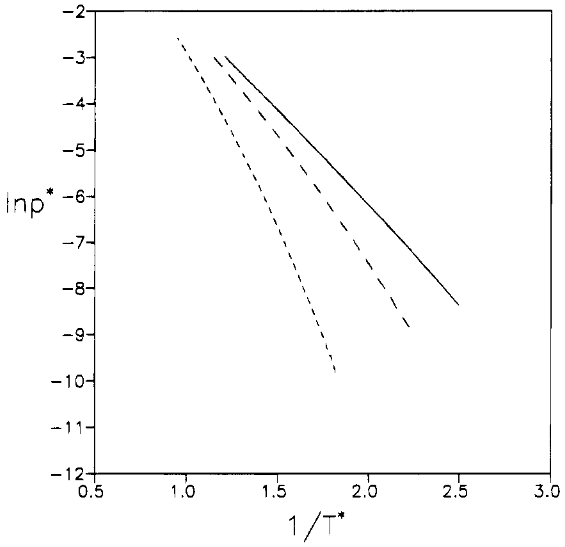

Figure 6. Vapor pressures of the liquid–vapor equilibria of linear quadrupolar models with $L^* = 0.3$ as obtained from the theory of this work: solid line, $Q^{*2} = 0$; dashed line, $Q^{*2} = 0.75$; short dashed line, $Q^{*2} = 1.5$. Reduced pressure and temperatures are defined by $p^* = p/(\epsilon/\sigma^3)$ and $T^* = T/(\epsilon/k)$.

Figure 7b. The results of Figure 7b suggest that there are two terms contributing to ω. The first arising from the short-range repulsive forces which are responsible of the molecular shape. The second arising from the attractive quadrupolar forces. All these facts are in good agreement with simulation results.[22] The calculated values of ω for quadrupolar models are also reported in Table 1. For $L^* = 0$ and $Q^* = 0$ a value of ω close to zero should be expected. We obtain however $\omega = -0.096$. This is probably due to the mean field approximation.

In Figure 8 we present the increase of the critical temperature defined by

$$\Delta T_c = (T_c - T_0) \tag{37}$$

for several elongations. In Figure 8a we plot ΔT_c versus Q^* as defined by eq 3. We also show ΔT_c as obtained from Gibbs ensemble simulations. The agreement between theory and simulation for ΔT_c is quite good. That may be explained from the fact that quadrupolar forces are treated with more accuracy than dispersion ones. Moreover, errors introduced by the mean field approximation seem to be constant with the quadrupole for a given elongation. According to Figure 8a, the same reduced quadrupole Q^{*2} provokes larger effects on spherical molecules than on anisotropic ones. However, when $\Delta T_c/T_0$ is plotted versus $Q^{*}_{eq}{}^{2}$ as in Figure 8b, we observe that the results fall approximately on a single line independently of L^*. Therefore, $\Delta T_c/T_0$ is weakly dependent on L^* and to some extent follows a single curve. This is observed in both theoretical prediction and Gibbs ensemble results from ref 22 so that it is clear that this is not an artifact of the theory. $\Delta T_c/T_0$ values for longer molecules are sligtly smaller than for spherical ones at a given $Q^{*}_{eq}{}^{2}$. The basis for this behavior follows from two different facts. The first is that the free energy at the critical point of a nonpolar model does not depend strongly on the elongation as can be seen from the last column of Table 1. The second is that A^Q along the critical isotherm of the nonpolar model does not depend strongly on L^* when the definition of eq 34 is used for $Q^{*}_{eq}{}^{2}$. This was shown in Figure 3. Therefore, surfaces formed by A^Q/NkT_0 (plotted as a function of density and temperature) for two different elongations are very close,

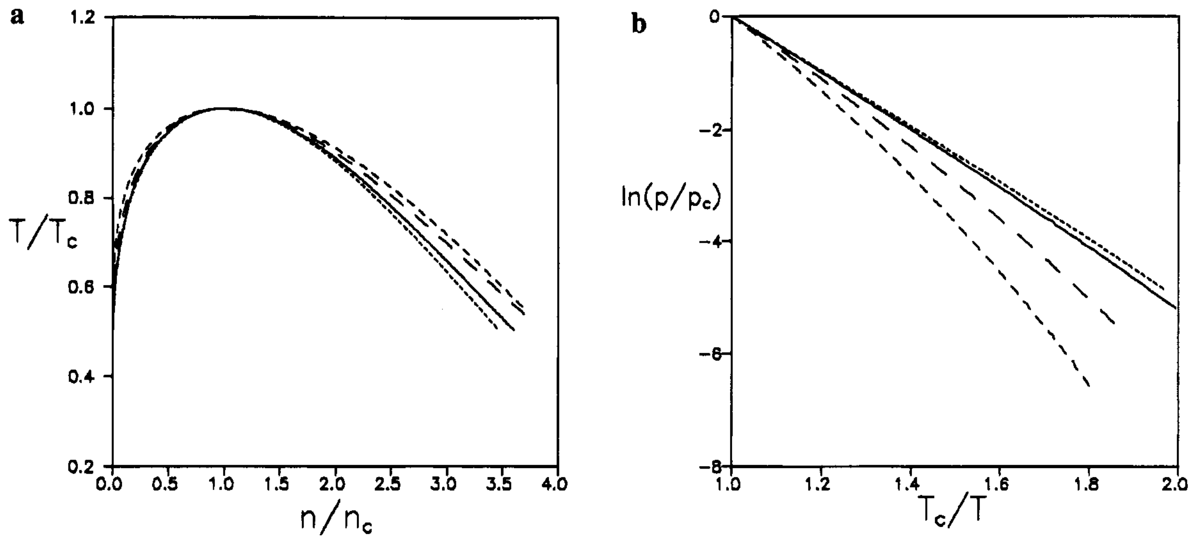

Figure 7. Corresponding states plot for linear quadrupolar molecules with $L^* = 0.8$ obtained from the mean field treatment of this work. Solid line stands for $Q^{*2} = 0$, long dashed line for $Q^{*2} = 1.49$, and dashed line for $Q^{*2} = 2.98$. Results for a spherical nonpolar model $L^* = 0$, $Q^{*2} = 0$ (short dashed line) are also shown. (a) Coexistence densities of the liquid−vapor equilibria. (b) Vapor pressure.

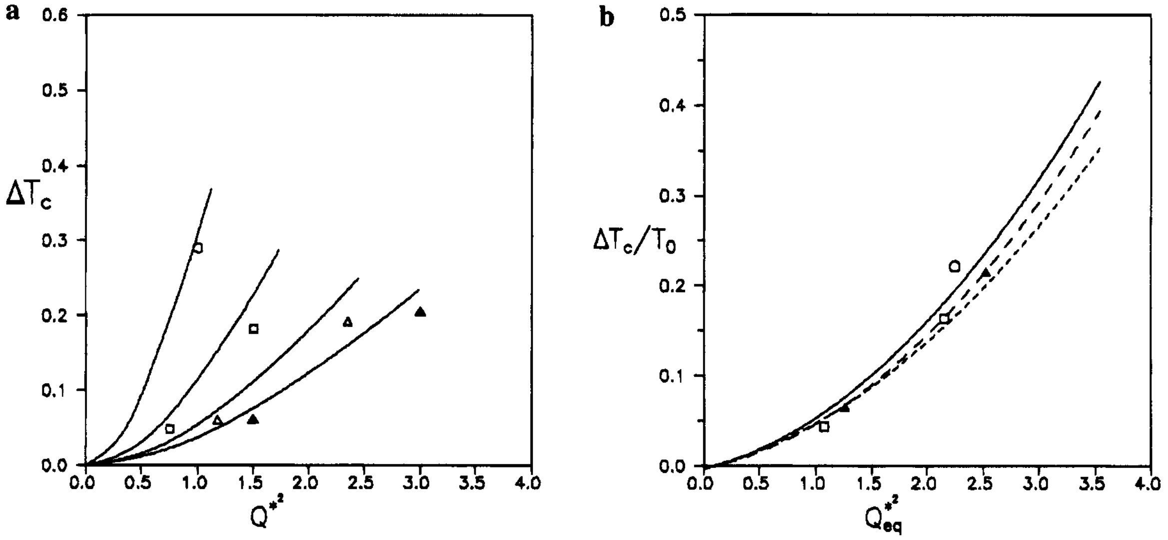

Figure 8. Increase of the critical temperature for linear quadrupolar model as obtained from the theory of this work (solid lines) and from simulation results of refs 22 and 11 for $L^* = 0$ (circles), $L^* = 0.3$ (squares), $L^* = 0.6$ (open triangles), and $L^* = 0.80$ (filled triangles). (a) ΔT_c (see eq 37) versus Q^{*2}. Solid lines are theoretical results. From the top to the bottom lines stand for $L^* = 0$, $L^* = 0.3$, $L^* = 0.6$, and $L^* = 0.8$. (b) $\Delta T_c/T_0$ versus the equivalent quadrupole $Q^*_{eq}{}^2$ defined by eq 34.

and one may expect quite similar changes on critical properties for two models with the same $Q^*_{eq}{}^2$. This is further illustrated from a more quantitative point of view in the next section.

The proximity between the free energy surfaces has another consequence. In Figure 9 we present results for $\Delta\omega$ defined by

$$\Delta\omega = \omega(L^*,Q) - \omega(L^*,Q=0) \qquad (38)$$

Results of $\Delta\omega$ for several elongations are shown in Figure 9. Again, the increase of the acentric factor due to quadrupolar forces does not strongly depend on L^* when models with the same $Q^*_{eq}{}^2$ are compared.

(C) Dipolar Models. The results for dipoles are in some respect similar to those presented for quadrupole models. In Table 2 we present results of the critical magnitudes. The dipole moment provokes an increases of the critical temperature, and this is common with quadrupoles. The critical density, however, behaves quite differently in dipolar and quadrupolar fluids. In dipolar fluids critical density increases very slightly with dipole moment, reaching a maximum and finally decreasing as the dipole moment takes higher values. This behavior differs from that observed in quadrupolar models where the quadrupole always provokes an increases of the critical density. Dubey et al.[21] have studied a two-center Lennard-Jones model plus a dipole (2CLJD). They found an increase of the critical temperature and a decrease of the critical density (high values of the dipole moment were considered in that work[21]) in good agreement with the theory of this work. Critical pressure from simulation[21] decreases with dipole moment. The theory of this work fails in describing this fact since it predicts an increase of the critical pressure with the dipole moment. As a consequence, the theory fails in describing the expected decrease of the compressibility factor due to dipolar forces.

Dipole reduces the vapor pressure at a given temperature and therefore provokes an increase of the enthalpy of vaporization. In Figure 10 we show a corresponding states plot for coexistence densities (Figure 10a) and vapor pressures (Figure 10b). We present results for $L^* = 0.3$. The presence of the dipole provokes a broadening of the coexistence curve. However, the effect is quite small, and dipolar forces seem to be less effective

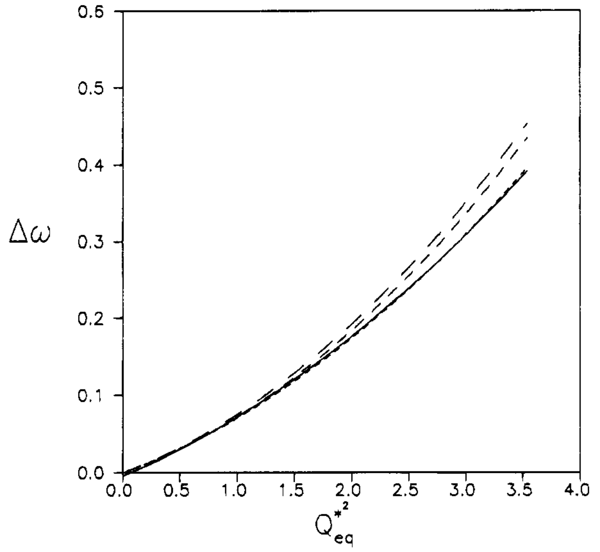

Figure 9. Increase of the acentric factor $\Delta\omega$ (see eq 38) as a function of $Q^*{}_{eq}{}^2$ for linear quadrupolar models of different elongations as predicted by this work: solid line, $L^* = 0$; long dashed line, $L^* = 0.3$; dashed line, $L^* = 0.6$; short dashed line, $L^* = 0.8$.

than quadrupolar ones in provoking the broadening of the coexistence curve. The dipole increases the slope (in absolute value) of the vapor pressure curve. Effects are similar to those found for a quadrupole moment. Again, from Figure 10 one may conclude that the acentric factor have contributions arising from the molecular shape and from dipolar forces. The results from our simple theory agree qualitatively with the results of more involved theories developed for 2CLJD.[13]

In Figure 11a we present $\Delta T_c/T_0$ defined by eq 37 for linear dipolar models plotted versus $\mu^*{}_{eq}{}^2$. The results follow a single line up to $\mu^*{}_{eq}{}^2 \simeq 1$. For larger dipole moment results depend on the value of L^*. The agreement with simulation results[40-42] is good. Spherical molecules present a larger increase in their critical temperature than nonspherical ones for a given value of $\mu^*{}_{eq}{}^2$. This can be understood from the results showed in Figure 3b. It can be seen that A_D along the critical isotherm of the nonpolar model increases (in absolute value) as the elongation decreases. Therefore, a higher increase of the critical temperature is expected for the spherical model. This is further illustrated in the next section.

TABLE 2: Critical Temperature T_c, Pressure p_c, and Density y_c of Linear Dipolar Models Obtained from the Mean Field Theory of This Work[a]

L^*	μ^{*2}	$\mu^*{}_{eq}{}^2$	T_c	y_c	p_c	ω
0	0	0	1.006	0.1304	0.090	−0.096
0	0.558	1.059	1.055	0.1318	0.096	−0.047
0	1.117	2.120	1.163	0.1322	0.107	0.008
0	2	3.796	1.372	0.1301	0.123	0.073
0	3	5.694	1.628	0.1256	0.138	0.118
0.3	0	0	0.823	0.129	0.050	−0.090
0.3	0.675	1.080	0.859	0.130	0.053	−0.053
0.3	1.345	2.158	0.934	0.129	0.057	−0.010
0.3	2.024	3.238	1.024	0.127	0.061	0.019
0.3	3.373	5.396	1.218	0.120	0.068	0.056
0.6	0	0	0.716	0.125	0.032	−0.078
0.6	0.797	1.118	0.745	0.126	0.034	−0.045
0.6	1.594	2.237	0.804	0.125	0.036	−0.010
0.6	2.391	3.355	0.873	0.122	0.038	0.013
0.8	0	0	0.666	0.123	0.025	−0.068
0.8	0.882	1.150	0.692	0.124	0.027	−0.037
0.8	1.764	2.298	0.744	0.122	0.028	−0.005
0.8	2.646	3.448	0.805	0.119	0.030	0.015

[a] The critical pressure is given in $p/(\epsilon/\sigma^3)$ units. Critical density is defined in terms of the packing fraction defined as $y = nV_m$. $\mu^*{}_{eq}{}^2$ is defined as $\mu^2/(kT_0V_m)$. Acentric factor is also shown.

In Figure 11b $\Delta\omega$ (defined analogously to eq 38) is plotted for dipolar fluids. The dependence with L^* is similar to that found for $\Delta T_c/T_0$. If the polar contribution to the pair potential is due to the dipole moment only, then spherical molecules present a larger change in the acentric factor than nonspherical ones for a given $\mu^*{}_{eq}{}^2$.

Before finishing this section, two observations are relevant concerning our linear dipolar model. First is that real dipolar diatomic fluids must be heteronuclear (the two atoms making up the molecule must be different in order to have a dipole moment), whereas the molecular core used in this work (a hard spherocylinder) is adequate only when the two atoms have similar sizes. Second is that molecules having a high dipole moment do also have an appreciable quadrupole moment (this is the case for instance of water). The case considered in this section applies only when quadrupole moment is negligible when compared with dipole moment. The study of dipolar heteronuclear models having both dipolar and quadrupolar forces although quite interesting is beyond the scope of this work.

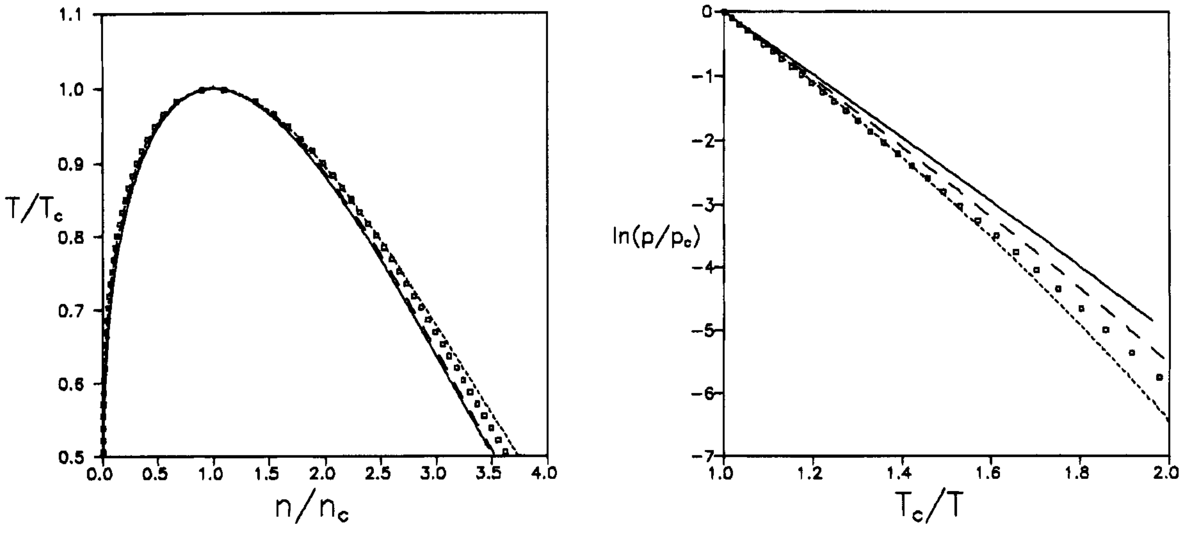

Figure 10. Corresponding states plots for polar molecules with $L^* = 0.3$. Long dashed line and symbols stand for dipolar models with $\mu^{*2} = 1.147$ and $\mu^{*2} = 3.373$, respectively. Solid and short dashed lines stand for a quadrupolar model with $Q^{*2} = 0$ and $Q^{*2} = 0.864$, respectively. (a) Coexistence densities of the liquid−vapor equilibria. (b) Vapor pressure.

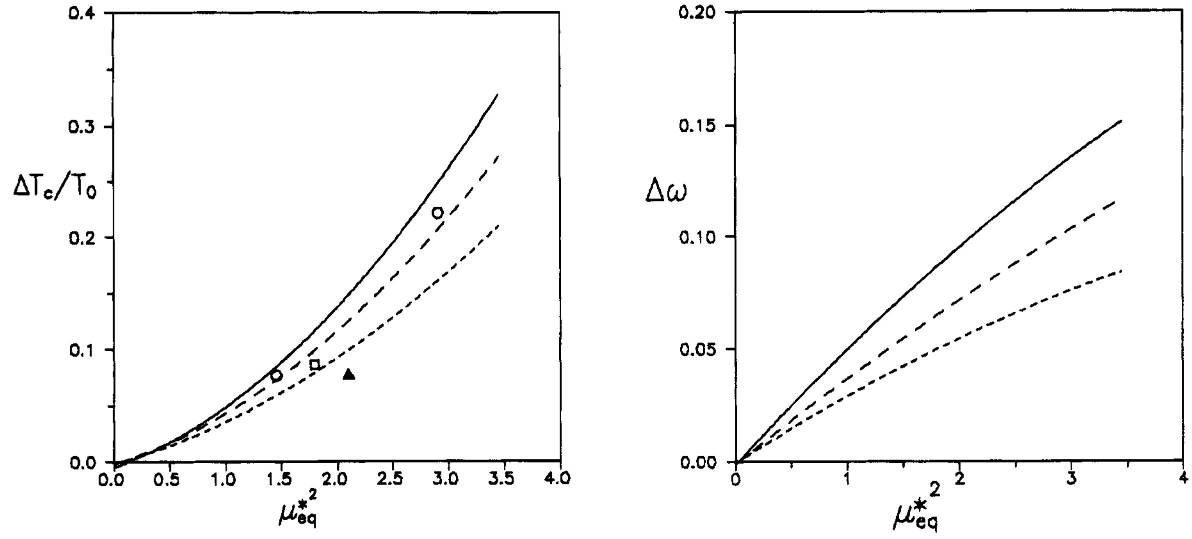

Figure 11. (a) $\Delta T_c/T_0$ (see eq 37 for ΔT_c) for linear dipolar models of different elongations as a function of $\mu^{*}_{eq}{}^2$. Theoretical results correspond to the solid line ($L^* = 0$), long dashed line ($L^* = 0.3$), and short dashed line for ($L^* = 0.8$). Symbols are Monte Carlo results from refs 40−42: circles ($L^* = 0$), squares ($L^* = 0.3$), and filled triangles ($L^* = 0.80$). (b) Increase of the acentric factor due to dipolar forces for $L^* = 0$ (solid line), $L^* = 0.3$ (dashed line), and $L^* = 0.8$ (short dashed line).

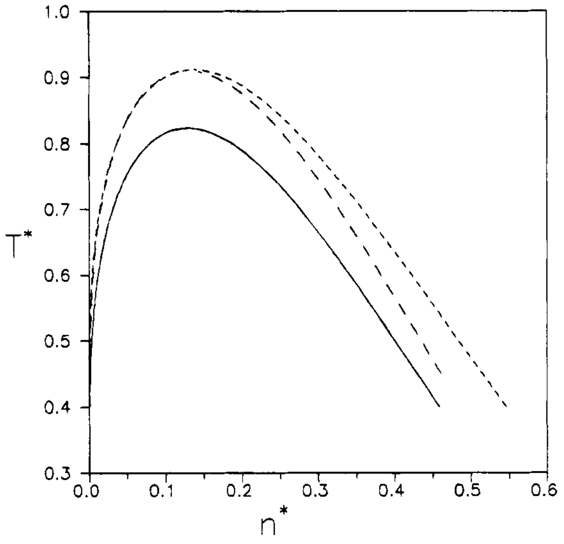

Figure 12. Liquid−vapor equilibria of a model with $L^* = 0.3$. Solid line corresponds to $\mu^{*2} = Q^{*2} = 0$, long dashed line to $\mu^{*2} = 1.147$, and short dashed line to $Q^{*2} = 0.864$. A corresponding states plot of these systems is also illustrated in Figure 10.

However, the dipolar model used here has an advantage. Since the molecular core used for the quadrupolar and dipolar model is the same (a hard spherocylinder), any discrepancy in the behavior of dipolar and quadrupolar fluids will be uniquely due to the different form of the dipolar and quadrupolar potential. In the next section such a comparison is performed.

(D) Quadrupole versus Dipole. Let us finish this section by presenting a comparison between the effect of a dipole or of a quadrupole on the phase diagram. In Figure 12 we compare coexistence densities for $L^* = 0.3$, when there is no multipole, when there is a quadrupole, and when there is a dipole present. We consider values of $\mu^{*}_{eq}{}^2$ and $Q^{*}_{eq}{}^2$ that provoke a similar increase of the critical temperature with respect to the nonpolar model. However, Figure 12 illustrates that dipole and quadrupole provoke different changes in vapor−liquid equilibria densities even when two models with the same critical temperature are compared. Dipole moment seems less effective than the quadrupole in broadening the coexistence curve. This is seen more clearly in Figure 10a where a corresponding states plot is shown for the three models shown in Figure 12. Figure 12 and Figure 10a illustrate an important point. If a dipolar and a quadrupolar model with the same elongation and critical temperature are compared, the quadrupole will present larger deviations from the principle of corresponding states. This is not only true for densities but for the vapor pressures as well (see Figure 10b). Quadrupole is more effective in increasing the slope (in absolute value) of the vapor pressure curve than the dipole. However, taking a higher dipole moment $\mu^{*}_{eq}{}^2 = 3.37$ and comparing with $Q^{*}_{eq}{}^2 = 0.86$ (see Figure 10), similar corresponding states plots from the critical point up to $T/T_c = 0.7$ are obtained. That guarantees that a four-parameter equation of state can simultaneously describe dipolar or quadrupolar fluids since it is possible to choose values of Q or μ that obey similar corresponding states plots.

Let us now compare the effect of a dipole or quadrupole on the critical temperature. By comparing ΔT_c for quadrupolar fluids (Figure 8b) with ΔT_c of dipolar fluids (see Figure 11a), it can be seen that for equal values of $\mu^{*}_{eq}{}^2$ and $Q^{*}_{eq}{}^2$ the quadrupole provokes a larger increase on the critical temperature. For $L^* = 0$ where there are results for quadrupolar and dipolar fluids this is what is observed in computer simulation.[40−43] There is another striking difference between the dipole and the quadrupole mentioned before. Whereas there is a weak L^* dependence in the plot of ΔT_c versus $Q^{*}_{eq}{}^2$ as can be seen in Figure 8b, this does not hold for dipolar models (see Figure 11a). Also, the critical density is modified in a different way by quadrupolar and dipolar forces. These results come out from the theory proposed here, but the reason of this different behavior is not clear. In the next section an explanation of these facts is proposed. Moreover, analytical formulas for ΔT_c and Δy_c (defined in an equivalent way to ΔT_c of eq 37) are provided. To achieve this goal, a simplified version of the mean field theory of this work is given.

V. Effect of Polar Forces on Critical Properties

In this section we derive algebraic expressions obtained from a still more simplified version of the mean field treatment of this work for the magnitudes $(T_c - T_0)/T_0$ and $y_c - y_0$. The total free energy of a polar system interacting through eq 24 is given by

$$A = [A^{HSP} - an] + A^{Q,D} \tag{39}$$

When no polar forces are present ($Q = \mu = 0$), the last term of eq 39 vanishes and the potential of eq 24 reduces to the Kihara potential. Therefore, the terms in brackets on eq 39 correspond to the free energy of a Kihara nonpolar model which will be denoted as A^{K} and eq 39 can be rewritten as

$$A = A^{\mathrm{K}} + A^{\mathrm{Q}} \tag{40}$$

From eq 40 we obtain for the pressure

$$p = p^{\mathrm{K}} + p^{\mathrm{Q}} \tag{41}$$

The critical point is obtained by solving the equations

$$p'(T,y) = 0 \tag{42}$$

$$p''(T,y) = 0 \tag{43}$$

where $p'(T,y)$ and $p''(T,y)$ are defined by the relations

$$p'(T,y) = \left(\frac{\partial p}{\partial y}\right)_{T,N} \tag{44}$$

$$p''(T,y) = \left(\frac{\partial^2 p}{\partial y^2}\right)_{T,N} \tag{45}$$

and where eq 42 and eq 43 hold at the critical point. Let us denote T_0 and y_0 as the critical temperature and density of a nonpolar model ($Q = \mu = 0$) with the same elongation that the model under consideration. The free energy of this nonpolar model is given by A^{K}. For any thermodynamic function $F(T,y)$ of the polar model a Taylor expansion can be performed around T_0 and y_0 to yield up to first order

$$F(T,y) = F(T_0,y_0) + \left(\frac{\partial F}{\partial T}\right)_y (T - T_0) + \left(\frac{\partial F}{\partial y}\right)_T (y - y_0) \tag{46}$$

Then by expanding the functions $p'(T,y)$ and $p''(T,y)$ according to eq 46 and taking into account that

$$\left(\frac{\partial p^{\mathrm{K}}}{\partial y}\right)_{T_0,y_0} = 0 \tag{47}$$

$$\left(\frac{\partial^2 p^{\mathrm{K}}}{\partial y^2}\right)_{T_0,y_0} = 0 \tag{48}$$

we finally obtain for eqs 42 and 43

$$T_0\left(\frac{\partial^2 p}{\partial T\,\partial y}\right)_{T_0,y_0} (T_c - T_0)/T_0 + \left(\frac{\partial^2 p^{\mathrm{Q,D}}}{\partial y^2}\right)T_{_0,y_0}(y_c - y_0) = -\left(\frac{\partial p^{\mathrm{Q,D}}}{\partial y}\right)_{T_0,y_0} \tag{49}$$

$$T_0\left(\frac{\partial^3 p}{\partial T\,\partial y^2}\right)_{T_0,y_0} (T_c - T_0)/T_0 + \left(\frac{\partial^3 p}{\partial y^3}\right)_{T_0,y_0} (y_c - y_0) = -\left(\frac{\partial^2 p^{\mathrm{Q,D}}}{\partial y^2}\right)_{T_0,y_0} \tag{50}$$

where T_c and y_c denote the critical point of the polar model. Equations 49 and 50 constitute linearized version of the mean field treatment of this work. They form a linear system with two unknowns $(T_c - T_0)/T_0$ and $(y_c - y_0)$. If we denote p_{Ty} and p^{Q}_{Ty} as

$$p_{Ty} = \left(\frac{\partial^2 p}{\partial T\,\partial y}\right)_{T_0,y_0} \tag{51}$$

$$p^{\mathrm{Q,D}}_{Ty} = \left(\frac{\partial^2 p^{\mathrm{Q,D}}}{\partial T\,\partial y}\right)_{T_0,y_0} \tag{52}$$

and we use a similar notation for the rest of the derivatives, then the solution of the system formed by eqs 49 and 50 is given by

$$(T_c - T_0)/T_0 = \frac{(p^{\mathrm{Q,D}}_{yy})^2 - p_{yyy}p^{\mathrm{Q,D}}_{y}}{T_0 p_{Ty} p_{yyy} - T_0 p_{Tyy} p^{\mathrm{Q,D}}_{yy}} \tag{53}$$

$$y_c - y_0 = \frac{T_0 p_{Tyy} p^{\mathrm{Q,D}}_{y} - T_0 p_{Ty} p^{\mathrm{Q,D}}_{yy}}{T_0 p_{Ty} p_{yyy} - T_0 p_{Tyy} p^{\mathrm{Q,D}}_{yy}} \tag{54}$$

Equations 53 and 54 can be applied to quadrupolar or dipolar fluids. All derivatives should be evaluated at T_0, y_0. The critical packing fraction of the nonpolar fluids y_0 are moderate. Then, instead of using the Padé approximant for $A_{\mathrm{Q,D}}$ in this section, we shall use the simpler expressions:

$$A^{\mathrm{Q}} = A^{\mathrm{Q}}_{2\mathrm{A}} \tag{55}$$

$$A^{\mathrm{D}} = A^{\mathrm{D}}_{2\mathrm{A}} + A^{\mathrm{D}}_{3\mathrm{B}} \tag{56}$$

In this way, $p^{\mathrm{Q,D}}$ and its derivatives are easily obtained. Moreover, eqs 55 and 56 yield similar results to the Padé approximant for not too high densities (as it is the case for y_0). In Figure 13 we compare $(T_c - T_0)/T_0$ as a function of $Q^*{}_{\mathrm{eq}}{}^2$ obtained from the mean field theory described in the main text and from the linearized version given by eqs 53 and 54. The agreement is quite good except at high quadrupole moments. The advantage of the linearized treatment is twofold. First, it yields algebraic expressions for the increase of critical temperature and density due to the quadrupole. Second, it allows an analysis of the factors determining these magnitudes.

In Table 3 we present results for the different derivatives appearing in eqs 53 and 54. We present results for two polar models of different elongation with the same $Q^*{}_{\mathrm{eq}}{}^2$ or with the same $\mu^*{}_{\mathrm{eq}}{}^2$. The denominator of eq 53 or 54 seems to be hardly affected by L^*, and this is true for dipolar and quadrupolar models. Let us focus therefore in the numerator of eq 53. For quadrupolar models the second term on the numerator of eq 53 does not change much with L^*. However, the term p^{Q}_{yy} decreases moderately with L^*. Since both the denominator of eq 53 and the second term of the numerator are rather insensitive to L^* in the case of quadrupolar models, the only L^* dependence is contained in the p^{Q}_{yy} term. That explains that for quadrupolar models $(T_c - T_0)/T_0$ is an almost universal function of $Q^*{}_{\mathrm{eq}}{}^2$ (see Figure 8b) although it is slightly smaller for more elongated molecules. In the case of dipolar molecules, however, the first term in the numerator of eq 53 is negligible in comparison with the second one. Moreover, the term p^{Q}_{y} presents an strong L^* dependence, and it decreases substantially with L^*. That explains the L^* dependence found for $\Delta T_c/T_0$ in the case of dipolar fluids. The decreases of critical density observed at high dipole moments is associated with the change of sign of the p^{D}_{yy} term (see last two rows of Table 3) which is negative for low dipole moments and positive for high dipole moments.

VI. Conclusions

A van der Waals theory for linear polar fluids has been proposed. Quadrupole moment increases the value of the critical

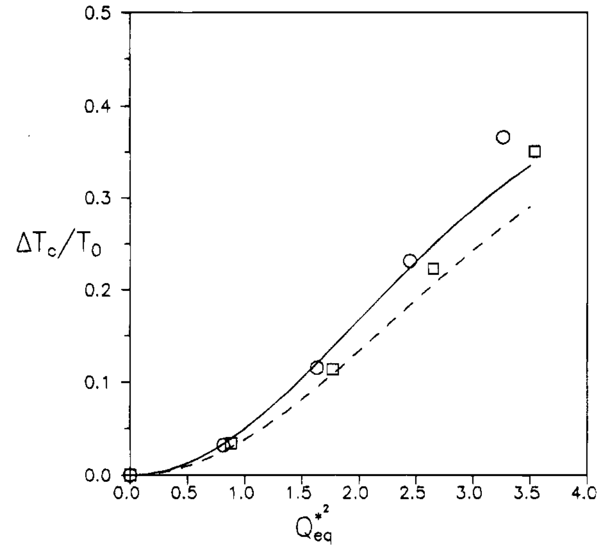

Figure 13. $(T_c - T_0)/T_0$ for quadrupolar linear fluids as a function of $Q^*_{eq}{}^2$. Lines stand for the linearized approximation of section V. Solid line $L^* = 0$ and dashed line $L^* = 0.8$. Symbols correspond to the complete mean field treatment of section III: circles ($L^* = 0$), squares ($L^* = 0.8$).

TABLE 3: Derivatives Evaluated at T_0, y_0 Required To Evaluate $(T_c - T_0)/T_0$ and $(y_c - y_0)$ According to the Linearized Mean Field Theory Proposed in Section V (See Eqs 53 and 54)[a]

L^*	$Q^*_{eq}{}^2$	$\mu^*_{eq}{}^2$	$T_0 p_{Ty}$	$p_{yy}^{Q,D}$	$T_0 p_{Tyy}$	p_{yyy}	$-p_y^{Q,D}$
0.0	2	0	3.92	−7.08	35.37	109.37	0.58
0.8	2	0	3.72	−5.72	34.43	134.03	0.45
0.0	0	2	3.32	−2.46	22.03	177.60	0.39
0.8	0	2	3.05	−0.68	19.97	206.25	0.22
0.8	0	3	2.59	3.40	1.405	308.19	0.26

[a] Results for quadrupolar and dipolar models are shown. For the notation see section V.

density, pressure, and temperature with respect to the nonpolar model. Dipole moment increases the critical temperature with respect to the nonpolar model. However, critical density increases slightly with the dipole moment, reaches a maximum, and then decreases for larger dipole moments. Critical density is therefore affected in a different way by quadrupolar and dipolar forces.

We propose a new way of reducing quadrupole and dipole moment. Using this new definition, we found the increase in critical temperature of quadrupolar models to be rather insensitive to molecular shape. For dipolar models the effectiveness of the dipole in modifying the critical temperature decreases with the molecular elongation. These two results can be understood from the behavior of A^Q and A^D at different elongations. Both observations are in agreement with recent computer simulation results.[22,42]

Polar forces provoke deviations from the principle of corresponding states. A broadening of coexistence densities (less pronounced for dipolar models) and an increase of the vapor pressure curve are observed when reduced by their critical magnitudes. We conclude that the acentric factor which is related with the slope of the vapor pressure curve has contributions from both molecular shape and polar forces. However, when comparing a dipole with a quadrupole provoking the same increase in the critical temperature with respect to the nonpolar model, it turns out that the quadrupole is by far more effective than the dipole in broadening the coexistence curve and increasing the slope of the vapor pressure. It is possible however, to choose a pair of values for the dipole and quadrupole moment so that they provoke similar deviations from the principle of corresponding states (at least for a certain range of temperatures).

The theory presented in this work provides a consistent and unified picture of the vapor−liquid equilibria of linear nonpolar, quadrupolar and dipolar fluids. Most of the predicted trends are in agreement with computer simulation results. Moreover, the theory provides a simple molecular insight in the behavior of nonspherical polar models. Two directions of improvement can be pointed out. First concerns the inclusion of new features in the Hamiltonian as hydrogen bonding,[44,45] heteronuclear cores, and simultaneous incorporation of dipolar and quadrupolar forces,[46] so that a better understanding of the vapor−liquid equilibria of real substances could be obtained. Second more rigorous theoretical treatments on linear polar models would be quite useful to test the trends predicted by the van der Waals-like theory of this work.

Acknowledgment. This work has been financially supported by Project PB91-0364 of the DGICYT. B.G. thanks Universidad Complutense by the award of a pre-doctoral grant. Helpful discussions with Prof. P. A. Monson are gratefully acknowledged.

References and Notes

(1) Van der Waals, J. D. Over de continuiteit van den Gas-en Vloestoftoes-tand. Thesis, Univ. Leiden, 1873.

(2) Rowlinson, J. S.; Swinton, F. L. *Liquids and Liquid Mixtures*, 3rd ed.; Butterworths: London, 1982.

(3) Cook, D.; Rowlinson, J. S. *Proc. R. Soc. London, A* **1953**, *219*, 405.

(4) Pople, J. A. *Proc. R. Soc. London, A* **1954**, *211*, 498.

(5) Shing, K. S.; Gubbins, K. E. *Mol. Phys.* **1982**, *45*, 129.

(6) Rigby, M. *J. Phys. Chem.* **1972**, *76*, 2014.

(7) Fischer, J.; Lustig, R.; Breitenfelder-Manske, H.; Lemming, W. *Mol. Phys.* **1984**, *52*, 485.

(8) Lombardero, M.; Abascal, J. L. F.; Lago, S. *Mol. Phys.* **1981**, *42*, 999.

(9) McGuigan, D. B.; Lupkowski, M.; Paquet, D. M.; Monson, P. A. *Mol. Phys.* **1989**, *67*, 33. Sowers, G. M.; Sandler, S. I. *Mol. Phys.* **1992**, *77*, 351.

(10) Vega, C.; Lago, S. *J. Chem. Phys.* **1991**, *94*, 310.

(11) Vega, C.; Lago, S.; de Miguel, E.; Rull, L. F. *J. Phys. Chem.* **1992**, *96*, 7431.

(12) Martin, C.; Lombardero, M.; Lomba, E. *J. Chem. Phys.* **1993**, *98*, 6465.

(13) Lupkowski, M.; Monson, P. A. *Mol. Phys.* **1989**, *67*, 53.

(14) Boublik, T. *Mol. Phys.* **1990**, *69*, 497.

(15) Boublik, T.; Vega, C.; Lago, S.; Diaz Peña, M. *Mol. Phys.* **1990**, *71*, 1193.

(16) Boublik, T. *Mol. Phys.* **1991**, *73*, 417.

(17) Vega, C. *Mol. Phys.* **1992**, *75*, 427.

(18) Bohn, M.; Fischer, J.; Haile, J. M. *Mol. Phys.* **1988**, *65*, 797.

(19) Saager, B.; Fischer, J.; Neumann, M. *Mol. Simul.* **1991**, *6*, 27.

(20) Panagiotopoulos, A. Z. *Mol. Phys.* **1987**, *61*, 813.

(21) Dubey, G.; O'Shea, S. F.; Monson, P. A. *Mol. Phys.* **1993**, *80*, 997.

(22) Garzón, B.; Lago, S.; Vega, C.; de Miguel, E.; Rull, L. F. *J. Chem. Phys.* **1994**, *101*, 4166.

(23) Möller, D. *Thermodynamik Fluider Mischungen : Kalorimetrie und Computersimulationen, Fortschrittbreichte VDI*; Reihe 3, Nr. 260; VDI-Verlag: Düsseldorf, 1991. Möller, D.; Fischer, J. *Fluid Phase Equilib.*, in press.

(24) Stell, G.; Rasaiah, J. C.; Narang, H. N. *Mol. Phys.* **1974**, *27*, 1393.

(25) Parsons, J. D. *Phys. Rev.* **1979**, *A19*, 1225.

(26) Vega, C.; Lago, S. *J. Chem. Phys.* **1994**, *100*, 6727.

(27) Boublik, T. *Mol. Phys.* **1992**, *76*, 327.

(28) Conroy, H. *J. Chem. Phys.* **1967**, *47*, 5307.

(29) Nezbeda, I. *Chem. Phys. Lett.* **1976**, *41*, 55.

(30) Saager, B.; Fischer, J. *Fluid Phase Equilib.* **1992**, *72*, 67.

(31) Müller, A.; Winkelmann, J.; Fischer, J. *J. Chem. Phys.* **1992**, *99*, 3946.

(32) Caillol, J. M. *J. Chem. Phys.* **1993**, *98*, 9835.

(33) Lado, F.; Lombardero, M.; Enciso, E.; Abascal, J. L. F.; Lago, S. *J. Chem. Phys.* **1986**, *85*, 2916.

(34) Paras, E. P. A.; Vega, C.; Monson, P. A. *Mol. Phys.* **1993**, *79*, 1063.

(35) McQuarrie, D. A. *Statistical Mechanics*; Harper-Row: New York, 1976.

(36) Kihara, T. *J. Phys. Soc. Jpn.* **1951**, *16*, 289.

(37) Boublik, T.; Nezbeda, I. *Collect. Czech. Chem. Commun.* **1986**, *51*, 2301.

(38) Saager, B.; Hennenberg, R.; Fischer, J. *Fluid Phase Equilib.* **1992**, *72*, 41.

(39) Pitzer, K. S.; Lippmann, D.; Curl, R. F., Jr.; Huggins, C. M.; Petersen, D. A. *J. Am. Chem. Soc.* **1955**, *77*, 3433.

(40) Van Leeuwen, M. E.; Smit, B.; Hendriks, E. M. *Mol. Phys.* **1993**, *78*, 271.

(41) Smit, B.; Williams, C. P. *J. Phys.: Condens. Matter* **1990**, *2*, 4281.

(42) Garzón, B.; Lago, S.; Vega, C.; Rull, L. F. Manuscript in preparation.

(43) Stapleton, M. R.; Tildesley, D. J.; Panagiotopoulos, A. Z.; Quirke, N. *Mol. Simul.* **1989**, *2*, 147.

(44) Jackson, G.; Chapman, W. G.; Gubbins, K. E. *Mol. Phys.* **1988**, *65*, 1.

(45) Jackson, G. *Mol. Phys.* **1991**, *72*, 1365.

(46) Benavides, A. L.; Guevara, Y.; del Rio, F. *Physica* **1994**, *A202*, 420.